A Minimal Pulsar[1] Detection System

or pulsar detection on a shoestring[*]

Peter W East

Introduction

In a previous paper[(2)] it was concluded that at least a 3m dish was required for detecting the strongest pulsars in both the North and South Hemispheres using the RTL2832U DVB-T dongle. Several amateurs (see, Neutron Star Group - Amateur Pulsar Detection[(3)] have achieved this aim with 3m and larger parabolic dish antennas and efforts have been made to construct antennas more suitable for a small garden. A. Dell'Immagine[(4)] has been successful at 422 MHz using a 3D corner reflector antenna with an aperture of 2 m by 2 m to intercept B0329+54. S. Olney[(5)] has successfully captured the Vela pulsar, B0833-45 in the southern hemisphere using a 5.7 m, circularly polarized 42-element crossed-dipole Yagi antenna at 436 MHz. Amateur detection of pulsars is not easy, the difficulties in this quest are well-documented[(6)]. With large aperture antennas, identifying pulsar signals can be achieved with some confidence but the challenge in this project[(7)] is to positively detect a pulsar with a small back-garden antenna when the integrated pulsar signal still competes with natural noise peaks.

In this note a pair of 2.5 m long, 17-element Yagi antennas (approximately 1.5 m^2 aperture) feeding three parallel RTL SDRs to cover the 608-614 MHz radio astronomy band is described, together with methods to identify and detect the B0329+54 pulsar at relatively low signal-to-noise ratios.

System Description

The radio astronomy frequency band 608-614 MHz was chosen for reasons of modest antenna size and having a wide beamwidth for long drift-scan acquisition times. Also, in addition to being in a region of reasonable pulsar signal levels, RF de-dispersion is not necessary in the chosen 2.4 MHz RTL SDR sub-bands. The system hardware largely follows the Quad RTL SDR Receiver outline suggested in Reference (8), except for the simplification of the noise modulation switch. A noise source is no longer required (see Figure 1) as the synchronizing function has been shown to be effective by modulating the receiver system noise.

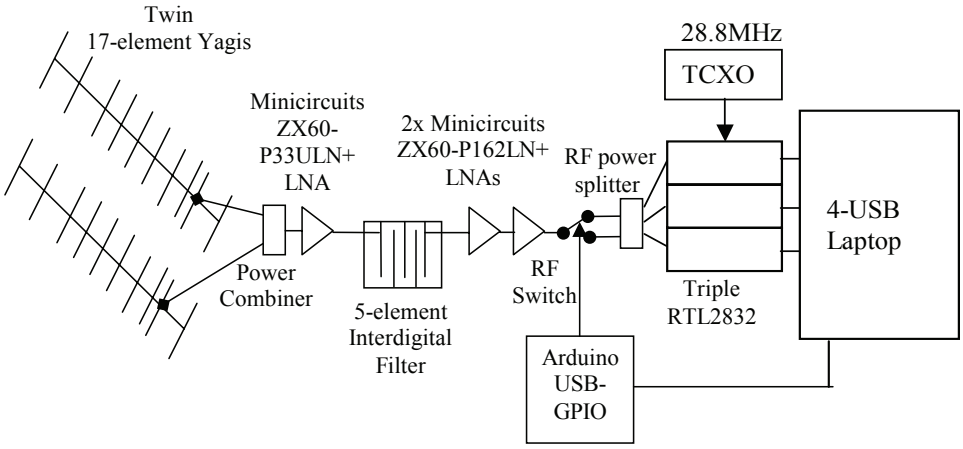

Figure 1. Pulsar Radio Telescope Schematic

The antenna developed for pulsar detection in the 611 MHz radio astronomy band is a twin 2.5 m long, 17-element Yagi. The design (Appendix 4) used the P. McMahon YagiCAD[(9)] design tool. The resulting structure using 1" aluminium box section boom and 6mm aluminium rod for the elements and fixed with self-tapping screws is light and portable and easy to construct. The twin-Yagi elevation and azimuth beamwidth is approximately 14° x 28° and oriented in drift-scan mode allowing for B0329 visibility between 3dB points of up to 3 hours. Yagis do suffer from high back and sidelobes and for this reason, at this frequency, a 1.4 m 3D corner reflector antenna with similar collecting area could have been chosen.

[*] Idioms Online: On or within a very tight or limited financial budget

The essential band-pass interdigital filter was designed using the online tool[10] by A. Changpuak. This calculator is particularly useful as it allows choices of box sizes, for instance the sides in this design (Appendix 5) were chosen as 25 mm by 6 mm (or 1" x ¼") for convenience of material purchase and ease of manufacture; the box and 6 mm copper rods are assembled simply using self-tapping screws (see Figure 2). M6 bolts are used for the tuning screws. The result is a band–defining filter with very sharp band edge cut-off and high out-of band Digital TV rejection. Cost of the aluminium metal for the construction of the antenna and filter was under $75 and construction time about a day each.

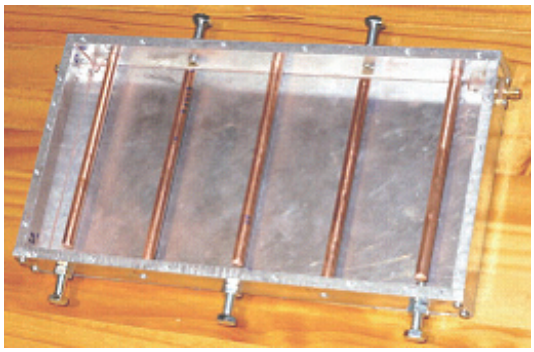

Figure 2. Antenna and Interdigital Filter Detail

Antenna: Two 17-element Yagi antennas with a theoretical combined gain of 19.3 dB and electrical cross-section of 1.6 m^2, mounted on a 1 m aluminium frame with a combined design beamwidth of 28° x 14°. The individual antennas can be oriented for vertical or horizontal polarization. For portability and convenience, they can be mounted and supported on a modified builders workbench. The RF 2-way reactive power combiner loss is less than 0.5 dB (Mini-Circuits ZAPD-21-S+).

RF Chain: One Mini-Circuits ZX60-P33ULN LNA (0.4 dB NF, 28°) + 5-element interdigital filter + 2x Mini-Circuits ZX60 P162LN LNAs (0.6 dB NF) + PIN diode RF switch (Mini-Circuits ZMSW-1211) + 4-way power divider.

Receiver: Quad RTL[8] assembly driven by a single 1 ppm TCXO and cooled with 4 fans. For the present tests, only 3x RTL SDR's are used at center frequencies 609, 611 and 613 MHz and each run with a 2.4 MHz clock. Gain setting is 33.6 dB. For better clock stability the SDR-Kits GPSDO can be set at 28.8 MHz allowing easier identification and match of pulsar topocentric[11] rotation frequency/period (the topocentric period of a pulsar is the observed rotation period as modified by the Doppler shift due to the Earth-pulsar relative motion).

PC: Dell Latitude D630 laptop with 4x USB ports running Linux.
Three USB ports link the 3 RTL units and the fourth port drives an Arduino USB GPIO card, which is used for controlling the PIN modulating switch.

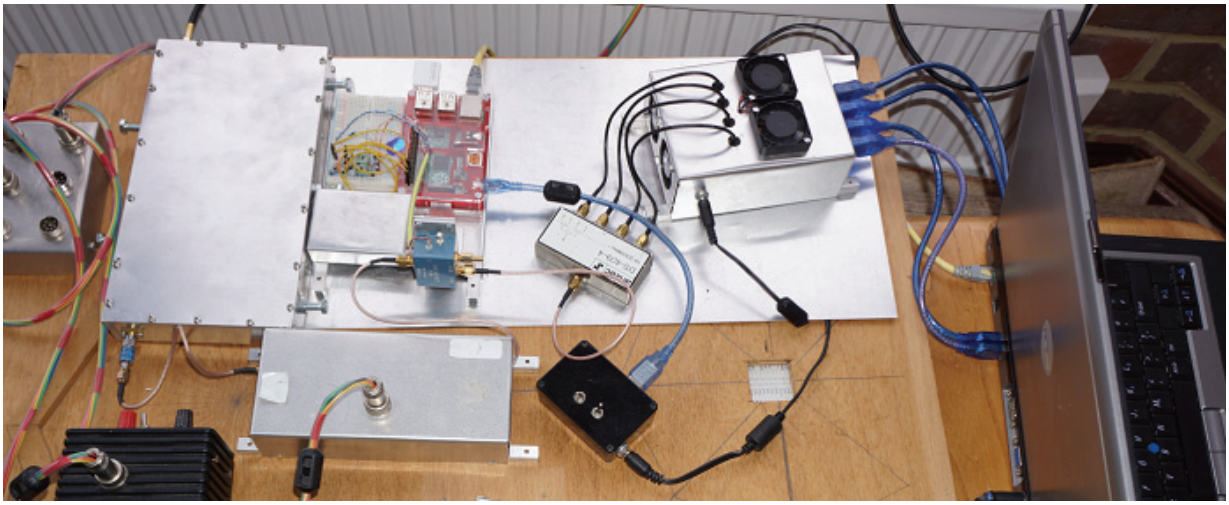

Figure 3. Receiving System Hardware

Figures 2 and 3 show the receiver hardware and layout. The construction is relatively simple and requires no special tools apart from a vertical drill and a vice. The band-pass filter and antennas can be set up using the 'USB 138M-4.4G Signal Source Signal Generator Simple Spectrum Analyzer'. Another useful RF tool is the modestly priced 'N1201SA UV RF Vector Impedance ANT SWR Antenna Analyzer'. Both are cheaply available on ebay.

Radiometer Equation and Sensitivity

To check that design has sufficient sensitivity, the well-known radiometer equation is applied. It is easily modified for the digital receiver case where data is ascribed to a fixed number of bins N and becomes,

$$\Lambda T = \frac{T_{sys}}{\sqrt{Bt / N}}$$

where, $T_{sys} = T_{receiver} + T_{sky} + T_{antenna}$
and, B is the RF Bandwidth, and t, the observation time.

In the present case, B = 6 MHz, t = 7500 s and N = 109 (optimum figure for pulsar B0329), so that $\sqrt{Bt / N}$ = 20,318

Analyzing a data measurement after folding, the mean DC level of the folded plot is equivalent to T_{sys} and the rms noise level equivalent to ΔT. The measured ratio for a typical trial test was 22000.

This close agreement indicates how effective the folding algorithm is in removing the effect of RF, video and spike interference. Although the observed interference level was low, some interference was clearly evident in the data. In early tests, software designed to remove interference prior to folding showed very little overall signal-to-noise ratio (SNR) improvement.

The folding algorithm, especially applied to very long records, becomes very finely tuned to the wanted period and will find strong peaks in random noise so that the pulsar validation routine must be very precise, especially when recovering low SNR pulsar signals; this is the major problem for small systems.

System Setup and Checking

The software package Radio Eyes[15] can be used to provide ephemeris data to correctly set the antenna pointing direction and set data acquisition times to collect data from the pulsar under investigation. In this instance the subject is pulsar B0329+54. At the author's location the pulsar peaks at due North at an elevation of 87.3°. Using Radio-Eyes to input the antenna beam pattern and pointing direction shows that the pulsar enters and leaves the antenna 3dB beam at an elevation of 76° and the optimum pointing elevation to maximize time in beam is 85.5°. An ex-military hand compass is used to set the north-pointing antenna direction.

To check the receiver system, the software, SDRsharp + Zadig driver from Airspy[16] can be used. The first check

is to monitor all three RTL SDR's in turn to check for similar power levels. Receiver noise temperature can be estimated by comparing the receiver output noise level with the LNA input open-circuited and loaded by a matched load since the expected noise power ratio with these arrangements is, ($T_{receiver}/(T_{receiver} + 290)$).

Given $T_{receiver}$, then T_{sys} can be estimated from the power received when the antenna is coupled and correctly directed.
Measurements using SDRsharp for the present receiver are;

LNA input open-circuit, p_{oc} = -23.2 dB;
LNA input connected to matched load, p_{ml} = -16.0 dB;
LNA input connected to match loaded power splitter, p_{mls} = -16.6 dB
Antennas connected via splitter, p_{rx} = -18.7 dB.

The SDRsharp software calibration is unknown, so these figures and those derived should only be taken as a rough indication, but it does allow a useful estimate of the system sensitivity.
From these figures, we can calculate:
$T_{receiver}/(T_{receiver} + 290) = p_{oc} - p_{ml}$ = -7.2 dB = 0.190 and $T_{receiver}$ = 68 °K
Including the power splitter, $T_{receiver'}/(T_{receiver'} +290)$ -> $p_{oc} - p_{mls}$ = -6.6dB = 0.219, so,
$T_{receiver'}$ -> 81 °K, showing a power splitter combining loss of just 15 °K or 0.2 dB.
Finally, the overall system noise temperature connected to the antennas pointed to the target direction is, $T_{sys} = T_{receiver'} + T_{sky} + T_{antenna}$ and is calculated from,
$T_{sys} /(T_{receiver'} +290) = p_{oc} - p_{mls}$ = -2.1 dB = 0.617 so, T_{sys} = 229 °K, or $T_{sky} + T_{antenna}$ = 148 °K.
These figures include cable loss between the antennas and combiner (say ~15 °K), but allowing 20 °K for the sky, still imply a strong contribution of antenna side and backlobes.

Applying the data presented in the radiometer section above, we can conclude that the system sensitivity, $T_{sys}/\sqrt{Bt/N}$, is approximately 0.01 °K. Assuming the antenna collecting area is around 1.5 m^2, this sensitivity is equivalent to 9 Jansky peak pulsar power, which is predicted to be sufficient to detect pulsar B0329+54 in a 6 MHz RF bandwidth centered on 611 MHz.
As a backup check the figures for the design were input to the S. Olney's online radiometer calculator[12]. The results are 10.4 J peak (single received polarization) with an expectation of a signal-to-noise ratio (SNR) using these figures of 4.0; very much supporting the approximate calculations made above.

Data Collection
Several C-programs have been written to facilitate data collection and processing; the sources are available for home compiling[13].
The three RTL SDR channels should ideally be switched on together to synchronize the recorded data. Unfortunately, although the three devices are controlled by a single batch file, software and PC operating system and hardware delays mean that there may be a few milliseconds difference in their switch-on times.
Data synchronizing is therefore the first task of the data processing. Synchronism is facilitated by operating the RF input switch with a random code to modulate the front-end noise simultaneously for all three RTLs for about 10 seconds. A separate Windows terminal triggers the modulation software simultaneously with the data acquisition software.

Acquisition Software:
The Arduino GPIO card is controlled by a Python program to randomly modulate the receiver noise at the start of the RTL SDR data recording.

RTL SDR data collection uses, *rtl_sdr22r.exe* which is a modified version of the Osmocom[14] software, *rtl_sdr.exe* and copes with producing very large files whilst switching off the inbuilt dithering. Also, the software written to initiate data collection and data modulation at the same time is, *run_prg_at.exe.*
The terminal commands (for detail see Appendix 1) with command parameters are:

Data collection, Terminal 1: *run_prg_at* "*rtlsdr.bat*" 20 30 00
Data modulation, Terminal 2 : *run_prg_at* "*python SwitchMod.py*" 20 30 00

To run the switch modulation program, Python 2.7 needs to be installed. The run time, <hr> <min> <sec> is user-chosen to encompass the time that the target pulsar is within the receiving antenna beam. Radio Eyes software can provide the expected time at beam center for these calculations.

Data Processing

Folding Algorithm Properties

The primary function of the folding algorithm is to cut the data up into sections equal in time to the expected pulsar period and add these together. In this way, the detected pulsar pulse aligns in position to add coherently and the base noise and interference power adds incoherently as the square root of the number of sections summed. Consequently, the pulsar amplitudes integrate and the pulse signal-to-noise ratio increases sufficiently to make the pulsar pulse visible.

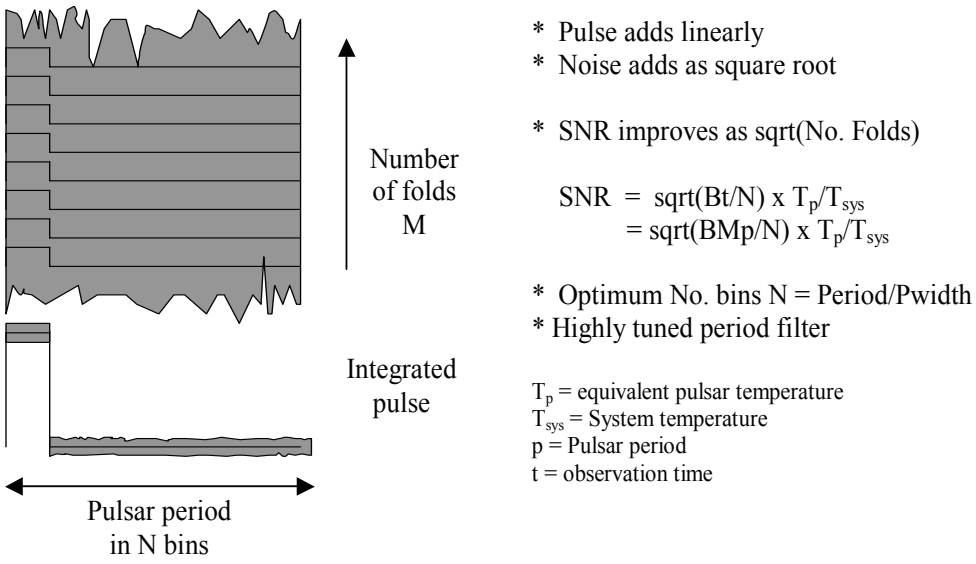

Figure 4. Folding Algorithm Summary

In frequency terms the operation can be thought of as applying narrow band filters about the harmonics of the pulsar fundamental frequency (= 1/period). This fine filtering property can and will find spikes and patterns in the residual noise or possibly RF interference of the right frequency that persist to generate ambiguous responses at random phases that compete with wanted low-level pulsar signal. Great care is therefore needed in validating suspected pulsar data at low signal-to-noise ratios.

Enhanced Folding Algorithm

A problem with applying the standard folding algorithm it that for larger bin numbers, less noise in the data record is averaged leading to a decrease in observed SNR and an increase of component noise frequencies. The increased noise frequencies add nothing to the pulse itself, as the pulse components are only a function of the pulse video spectrum; so removing them should lead to an improved SNR. There are various ways to filter a standard folded file and the one chosen for easy adjustment involves convolution. By multiplying the folded data spectrum by a similar target pulse spectrum and then inverting the resulting spectrum product; the folded result becomes exactly matched to the expected pulse shape. Excess high frequency noise is removed and an improved SNR results. At optimum, the pulse shape and delay are not compromised. A Gaussian shaped target of about half the width of the expected pulsar pulse gives very good results. The technique appears to maintain the optimum SNR of the standard algorithm (which occurs when the number of bins equals the ratio: period/pulse width) for all bin numbers allowing much finer pulse resolution and detail to be observed.

Processing Software *(see Appendix 2)*

The very large binary files produced by the three RTL SDRs contain in-phase and quadrature samples at the RTL clock rate (>2 MHz) that can be processed directly in raw .bin form by correlation, de-dispersion and folding software. In the case of pulsar B0329 it is possible to downsample and detect the running average amplitude at a sample rate of 1 kHz and carry out data correlation/synchronizing prior to folding. The downsampling effectively reduces the processing time of subsequent software functions.

Within-band de-dispersion processing can be avoided in this design as, at 611 MHz, the pulse dispersion in a 2.4 MHz bandwidth is small (2 ms) compared to the pulsar pulse width (6.5 ms) and so de-dispersion has little effect of improving detectability and pulse fidelity. Band-to-band de-dispersion is necessary however, and can be carried out by the simple process of applying suitable relative time-shifting to the detected band files before combining.

Detection Software:

The software: *pdetect22.exe* operates on the raw .bin files (typically 36GB each) and carries out sample amplitude detection and down-sampling of the binary data files to produce smaller text data files. This initial downsampling is usually of the order 1000, ensuring much reduced post processing times.

Correlation software:

Correlation software, *cor_tim1_nv.exe* compares the initial modulation of pairs of detected *pdetect22* text files corresponding to the pairs of receiver band channels to determine offsets between the actual band start times. The offsets guide the file trimming process using *txttrim.exe* to synchronize the three band data. The initial modulation range also needs removing and the data files trimmed accordingly. Once the three files are trimmed taking into account the adjustment required for de-dispersion, the files can be summed using *filesum2.exe* for the following folding process.

Folding software:

The folding software, *rapulsar2_avg2conv.exe* incorporates the SNR enhanced fold algorithm and operates on the summed 3-band output text file. The output text file is suitable for display using Windows Excel or alternative spreadsheet software.

An alternative processing method if available is to employ a Math CAD suite. Here, a MathCad 2000 program, *DataCheck.mcd* has been developed to align and fold the three band downsampled data files. It facilitates synchronising, trimming, de-dispersing and summing files suitable for detailed investigation. Unfortunately the CAD program is limited to files of 8 MB samples which may limit the application. The program is detailed in Appendix 3 and could be transcribed for Matlab or any other Math CAD programs.

Validation Software:

DataCheck.mcd – For validation, functions are included (Appendix 3) for simultaneous checking of file first/second half correlation, multiple period folding correlation, band correlation and period search and dispersion optimization. Trial 31 is used as an example. Final validation is effected by running *DataCheck.mcd* and testing for expected effects in positive and negative dispersion realms.

Example Results - *Dataset 24* (*See Appendix 3 for MathCAD results of Dataset 31*)

Trial No: 24 was carried out on 07/08/2017. The observation time was ~ 7500s around culmination at 86° elevation. Antenna elevation beamwidth 14° set at 84° elevation. Azimuth pointing direction set at 0°.

As an initial check; the measured detected mean-to-folded rms noise ratio was >20000 = $(T_{sys} + T_{sky})/\Delta T$, indicating that ΔT is of the order 0.01°K. A SNR of 3 is therefore equivalent to a pulsar temperature of 0.03 °K.

Assuming an effective antenna capture area of 1.5m^2, the Jansky peak equivalent is around 27 J or 0.24 J mean. (from $T = JA/1380$) This compares to the published data of up to 0.4 J for a single polarization.

In the following plot, the raw data was downsampled, detected and output at a clock period of 1 ms. The pulsar candidate is set at bin number 55 of 109 bins.

Topocentric period error for best SNR is -0.375 ppm, which is well within the expected 50% range of ±1.8 ppm, bearing in mind the tolerance of the TCXO used is only 1ppm.

Figure 5a shows the final result of folding the summed 3-band data, optimally moving the maximum to the center of the center bin by adjusting the initial system clock offset and fold period. The SNR is calculated using all the data outside the bin maximum to determine the data mean and rms.

Comparing Figures 5a and 5b illustrates the improved detail using the enhanced folding algorithm using 715, 1 ms bins. The advantage of many bins whilst maintaining optimum SNR is evident in period searching as the peak response does not suffer from power loss/division at the coarser bin boundaries.

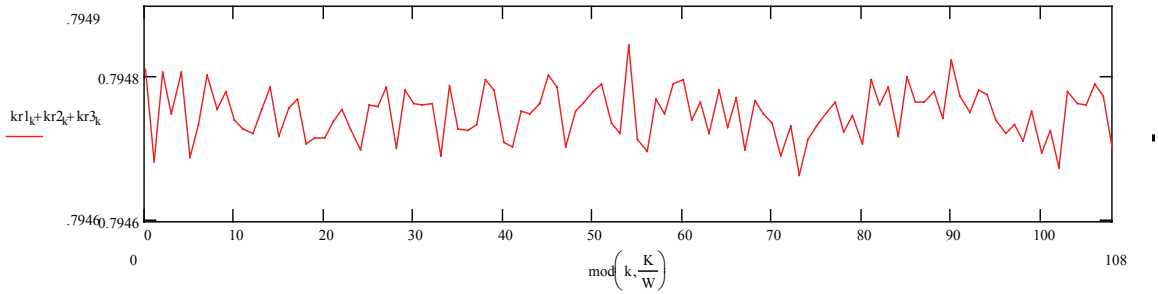

Figure 5a. 3-Band De-dispersed Final Result SNR = 3.0 (109x6.6 ms bins)

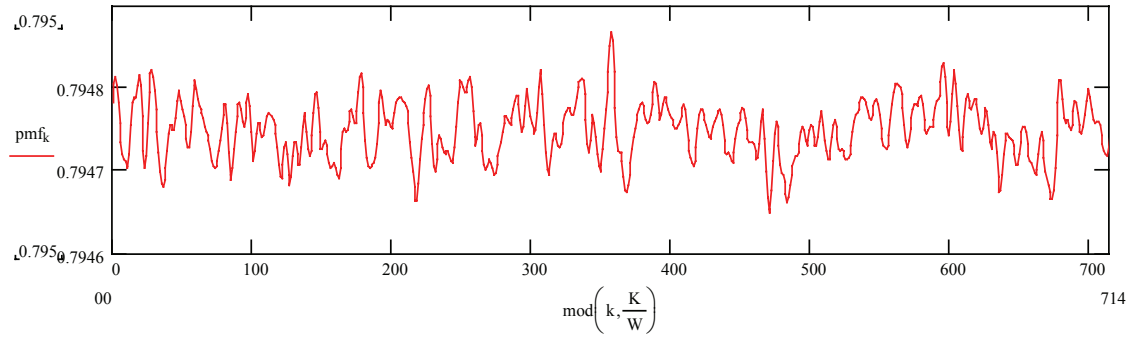

Figure 5b. Enhanced Fold Algorithm, SNR = 3.1 (715x1 ms bins)

Preliminary Search and Validation

In small aperture pulsar detection systems, even very long-time data records may only produce detected SNR's of maybe only 2 to 5. Since the expected range of Gaussian noise peaks is in this region, there will always be some ambiguity in identifying a true pulsar pulse. So an extreme validation routine is necessary. Folded noise peaks can masquerade as pulsar-like signals and are a source of erroneous detections. All of the tests described can fall foul of noise/interference impersonations and pulsars themselves at this level do not have a 100% discriminating property.

Initially, a preliminary check on data quality for acceptable RFI on downsampled amplitude-detected data should be made, then, band data aligned, bands de-dispersed, combined and initial drift, RF spikes etc: removed or nulled as described in the 'Processing Software' section above.

The combined file can then be inspected by running the folding software using the topocentric period ±0.5 ppm. If a pulsar is present then a correlating pulse will appear in the folded comparisons. The period can then be optimized followed by a selection of the validation tests below.

A recommended validation routine after candidate identification and period search to confirm identity comprises the tests…

1. Candidate topocentric frequency within an acceptable range versus the receiver clock accuracy.
2. Candidate correlation between data file sections.
3. Candidate correlation of multi-period folds.
4. Candidate correlation between receiver bands.
5. Pulse width and shape confirmed.
6. Confirmation of typical scintillation over the observation period and between bands.
7. Correct time shift, amplitude and width spread confirmed with ppm period search.
8. Correct time shift, amplitude and width spread confirmed with de-dispersion variations.

A true pulsar will pass all validation tests and show day-to-day consistency.

Once positively identified, daily records can be added to provide improved SNR and indication of pulse detail.

Test 2

For each chosen search period, a plot such as Figure 6 shows the correlation between the two halves of the data file (first half red, second half, blue) of the 3 bands combined data file; each half is folded separately. Strong correlation may be evident at the correct search period, as shown here at the central bin. There are other obvious regions where 'noise' peaks closely align and these must be noted and judged, based on following tests. Initial red/blue peak alignment occurs as a function of the Test 1 selected fold period, and further investigated in Test 7.

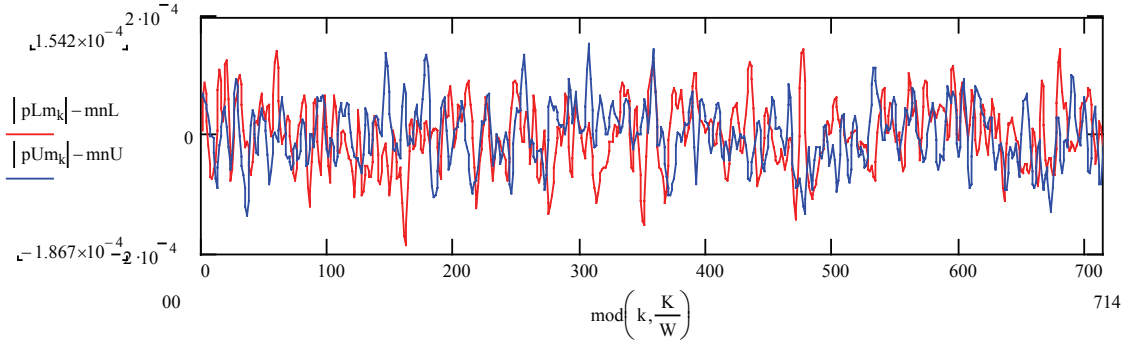

Figure 6. First half file v second half file correlation, SNRs = 2.5, 2.3

Test 3

Figure 7 shows the multi-period fold response of the summed 3-band detected data file, again showing strong correlation and pulsar pulse presence at the expected central bin. For this triple-period folded presentation, the second pulse period and third periods have been overlaid on the first to demonstrate central bin pulse coincidence, again in the Test 2 - adjusted central bin.

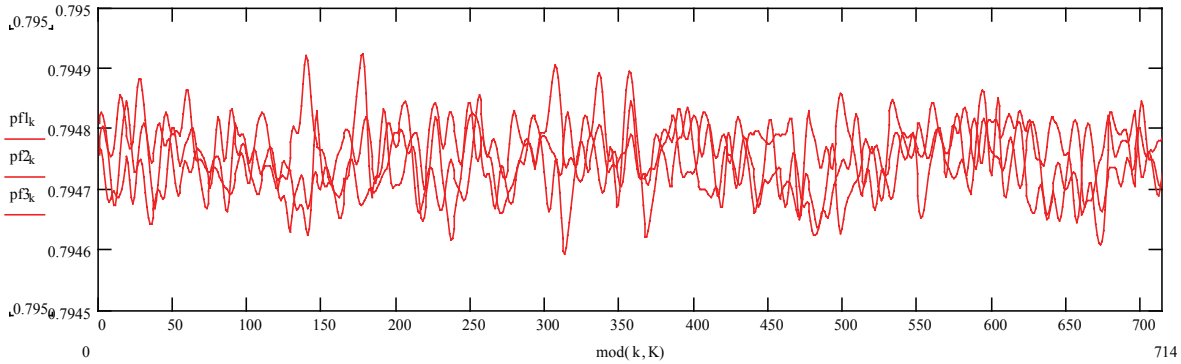

Figure 7. Triple Period Correlation

In this test the fold period is exactly 3-times the optimum pulsar period. In overlaying the three single period fold sections, the pulsar pulses overlap and to a certain extent, the inter-pulse noise sections show little correlation. At this point false Test 2 candidates can also be checked.

Test 4

Figure 8 plots the correlation between the three bands folded individually and shows a positive correlation of the 3 separate band responses at the expected central bin.

This test is quite strong, as being different frequency bands, the base noise must be uncorrelated and allowing for different scintillation effects, the pulsar is still expected to appear in all bands. There is of course, still a random probability of coincidence. Note the lower signal-to-noise ratios for the individual bands.

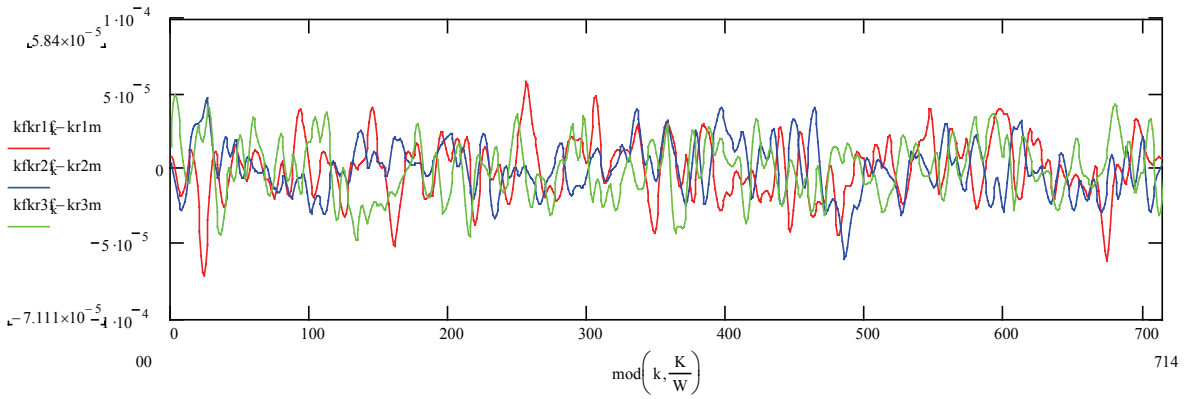

Figure 8. Band-to-band correlation - SNRs = 1.6, 1.8, 1.9
(red: 609 MHz; blue: 611 MHz; green: 613 MHz)

Test 5

The pulse width and shape are evident in comparison with a 6.5ms Gaussian-shaped pulse as shown in Figure 9. There appears to be some obvious noise distortion, which might be expected at low SNR.

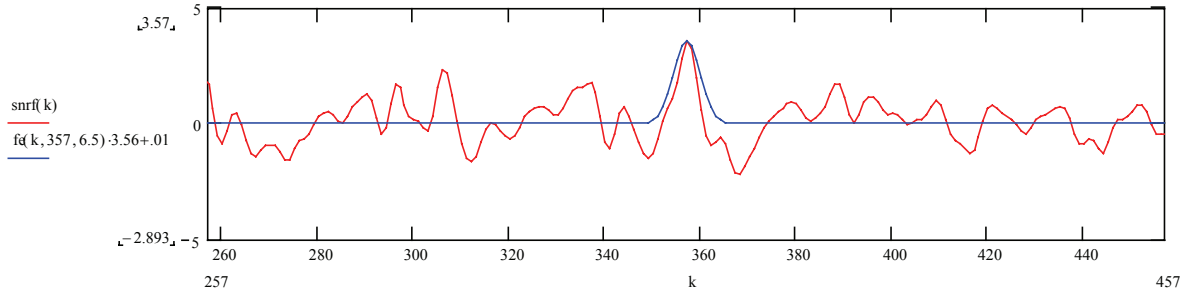

Figure 9. Pulse Width Plot (ms)

Test 6

The figure below shows the indicated SNR in each band over 30min time slots of the total record. The blue curve shows the summed version showing that less variation than the individual bands. As expected band scintillation is uncorrelated but appears to be present.

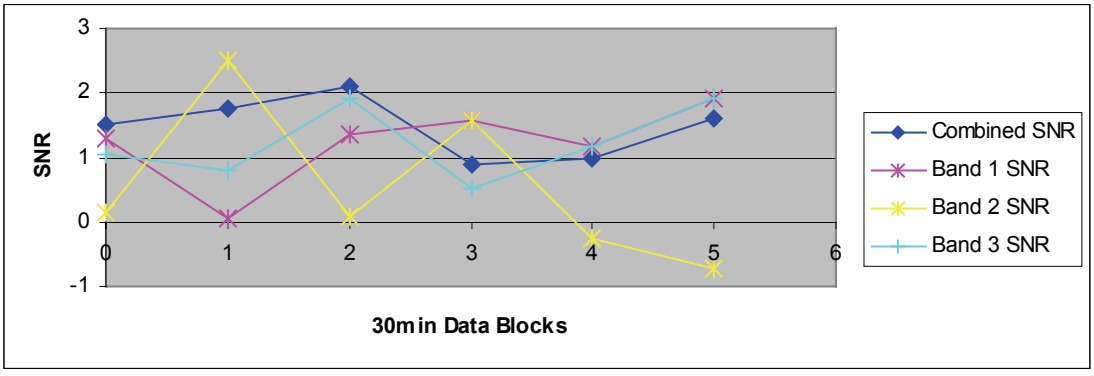

Figure 10. Scintillation

Test 7

The usual method of tuning the test period, when folding to identify the pulsar peak, is to change the period in a few parts per million steps to look for a regular fall-off either side of the matching period. With weak signals and using the 'optimum' number of bins, this can be difficult as the relative position of the pulsar peak varies with power being shared between bins and also the peak varies as a function of the period. These problems are of less

importance when enhanced folding is used to improve resolution. However, accurate pulse position movement, amplitude and width, can all be predicted to confirm the pulsed nature of the wanted signal.
Consider, if T is the data record duration and P the pulsar period and t the pulse position offset from the file start, then changing the period by $+p$ parts-per-million (ppm), the first pulse start position changes to $t\text{-}pP$ and the last pulse folded position to $t\text{-}pT$.
So when completely folded, the mean/pulse center shift is $-pT/2$ and the pulse extent increases to pT.
The plot below summarizes the expected pulse width, amplitude and pulse center position changes as a function of the period change in ppm times the data duration/pulse width. The model used to derive the plots below, assumes a Gaussian-shaped pulse with half-height equal to the wanted pulsar pulse width. Attendant noise may, of course impose uncertainty on these predictions, but what we are looking for is consistency over a range either side of the initial set period; the half-height width of the stretched pulse can now be predicted and is a positive aid in validation.
The match peak occurs naturally when there is no period error, but it is interesting to note that the pulse amplitude drops to 0.5 when the period error times the data observation duration exceeds twice the expected pulsar pulse width. This is a useful pulsar test and may be used to discriminate from false candidates.
Perfect matching to this theory cannot of course be expected due to the influence of finite residual noise and of course the effects of scintillation during the record.

It is interesting to consider what folding does to the background noise. In fact the noise resultant comprises the residual periodicities that the intense folding finds in the background noise. Some may arise from RF interference or noise features that persist for long periods in the data record. As such some noise peaks may display similar properties to pulsar pulses and be a source of confusion. However, in most cases, the position shift of false candidates with period change may not always equal that expected of a true pulse.

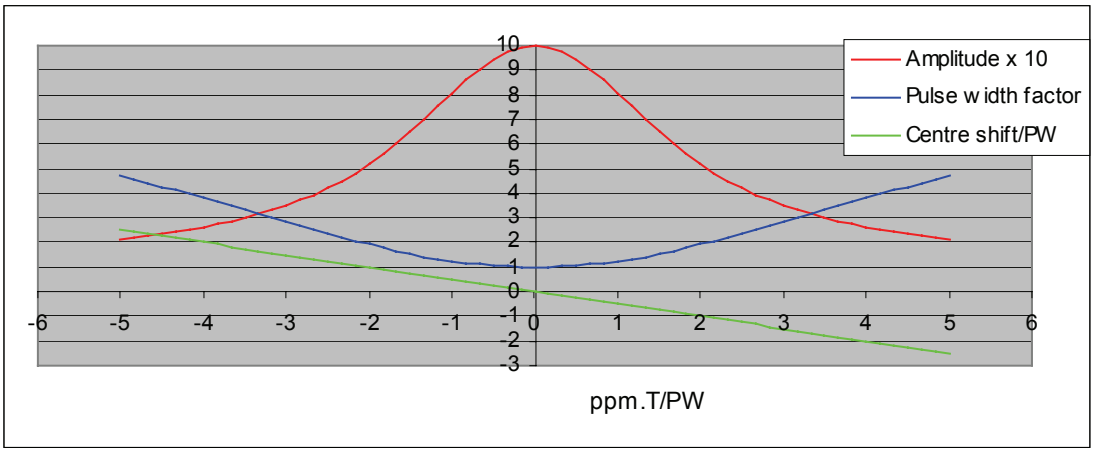

Figure 11. Period Search Amplitude, Position and Pulse Width Predictions

The plot in Figure 12 below the red curve is a peak SNR of about 4.5 from Dataset 35. The other plots are the responses at 0.5ppm period search steps. i.e. blue is + and -0.5ppm (green ±1 ppm, etc for magenta, cyan, brown). The x-axis is in 1/3 ms increments using an enhanced fold algorithm with 2143 bins. The black curve is the calculated amplitude response assuming a Gaussian-shaped pulse of 6.5 ms half height. The expected increment change is calculated as $pT/2$ = 3.8 ms/ppm, where p is the ppm change and T the record length = 7600 seconds. Actual measurement of the plot peak differences give a variation 3.8±1.0 ms.
Obviously there are some effects within the pulsar peaks due to the underlying noise.
An interesting observation to note is that the noise peaks outside the pulsar position also move and change with pulsar period change and there seems to be some correlation, certainly with the smaller increments.
For this to happen it means the residual noise peaks must be present and correlate within the pulsar period over a large part of the data record. This might be expected as this is just what the folding algorithm is meant to do and is the reason for ensuring the validation process must reject these false candidates. They invariably fail the amplitude curve match criterion as the chance of the noise spikes matching the target pulse width is probably low.
The central part of the plot has been expanded to improve visibility.

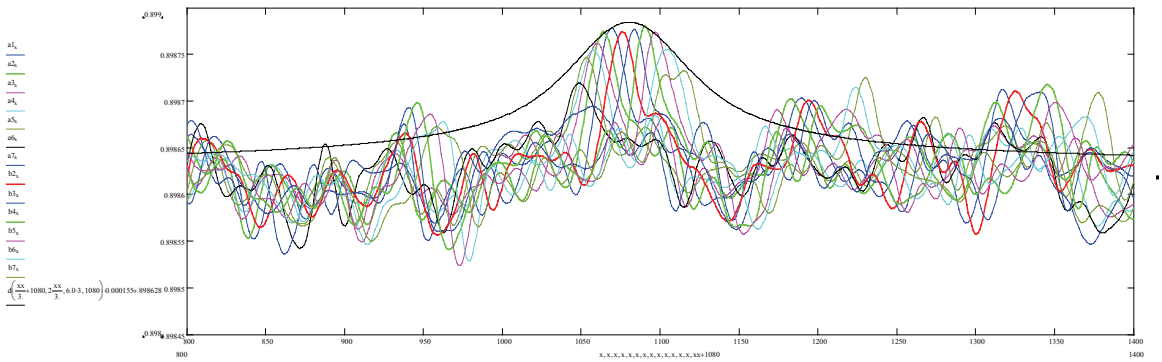

Figure 12. Period Search Amplitude, Position and Pulse Width 0.5ppm increments

Test 8

The dispersion property of pulsar signals is considered the prime identifier and adds maximum weight in verification.

In this section, dispersion variation is defined as the frequency delay in ms/MHz times the receiver bandwidth in MHz over and above that normally required to de-disperse the pulsar pulse.

The effects of positive or negative extra-dispersion on a pulsar pulse begin to be noticed when the magnitude of the total dispersion in ms across the band approaches the pulsar pulse width. At this point, the dispersed pulse width slightly increases and the amplitude drops by 15-20%. For larger dispersion delays, the pulse width increases to equal the delay. The amplitude drops by 50% when the band dispersion equals twice the pulse width. The expected changes based on a Gaussian pulse shape are illustrated in the following plot. This idealized situation may be observed with large SNR pulsar signals but will be obscured somewhat by noise at low SNR's; however, trends should still be present to aid data validation.

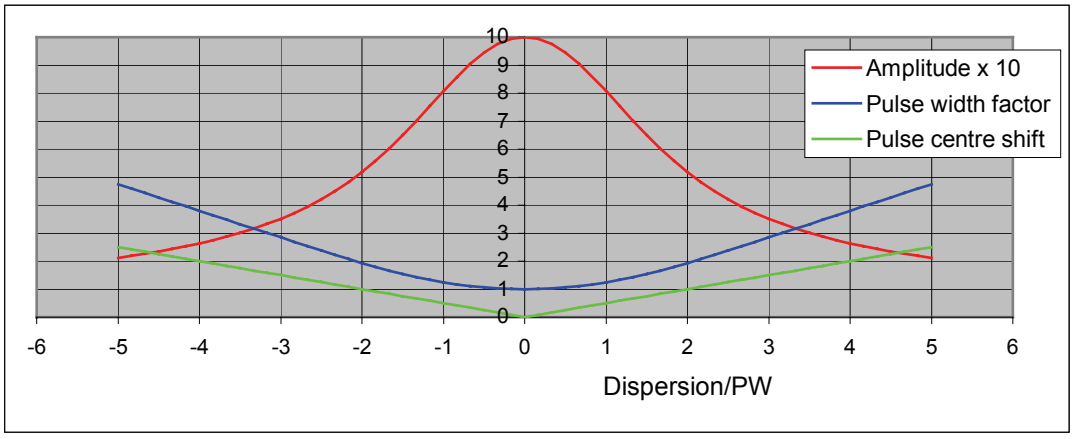

Figure 13. Dispersion Search Amplitude, Position and Pulse Width Predictions

The two plots below (Figure 14) show the result of folding a half file of data record (Dataset 35), with negative and positive band over-dispersion respectively relative to the 609 MHz band. It is evident that, as the dispersion match degrades, the pulse amplitude decreases and the pulse width increases in both cases. The left hand scale gives a measure of the instantaneous SNR and the x-axis here is in 1ms increments.

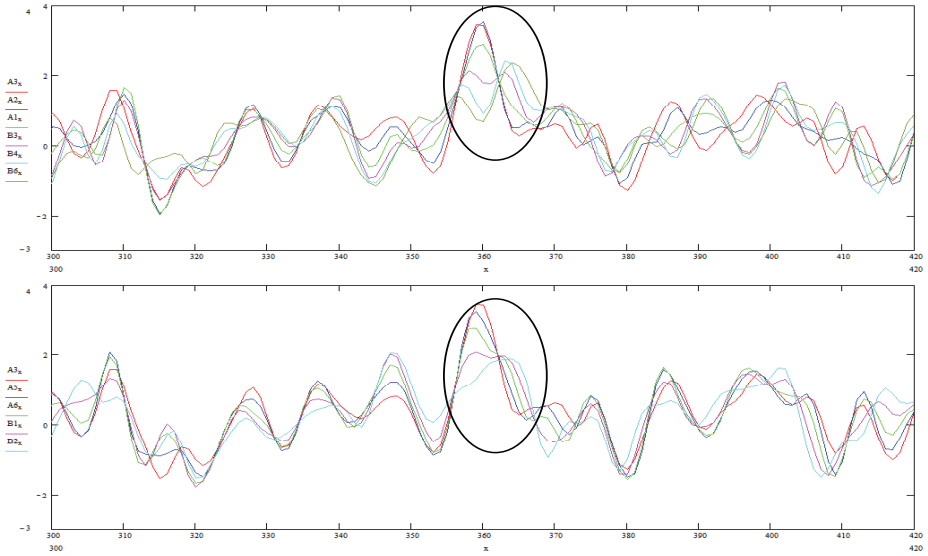

Figure 14. Dispersion Search Measurements

The plot below shows the measured results from Figure 14 plotted with the expected amplitude and pulse width responses, assuming a Gaussian-shaped pulsar pulse.

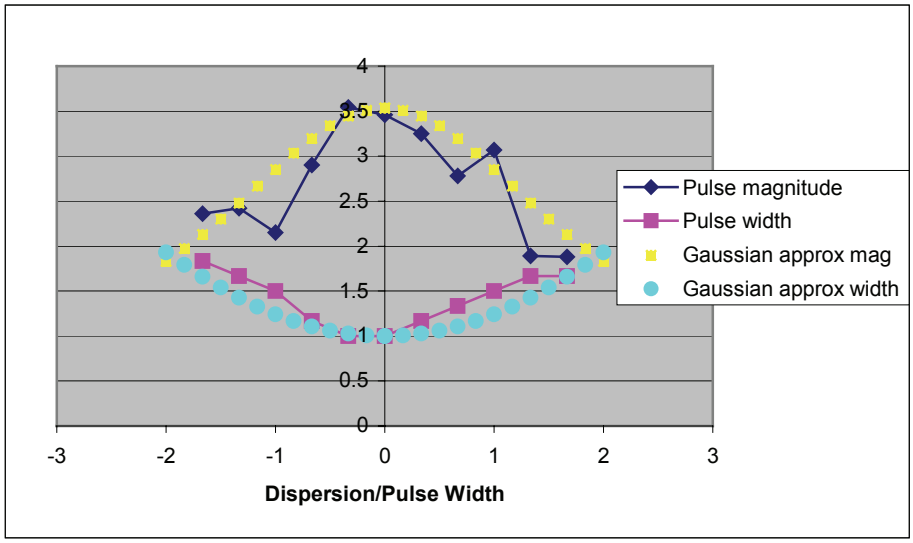

Figure 15. Dispersion Search Measurements Summary

The positive match between measurement and simple theory is remarkable, bearing in mind the pulsar peak SNR in this second half of Dataset 35 is only 3.5 so noise corruption is expected but the serious scintillation of B0329 is likely to also distort the dispersed pulse shape. To overcome the scintillation problem, care was taken to select a section of data that appeared to be equally strong in the three receiver bands.

Conclusions

Detection of the B0329+54 pulsar is possible using a basic receiving system based on a home-made Yagi pair antenna and TCXO-driven RTL2832U DVB dongles with relatively cheap RF LNA amplifiers as described. There is no doubt that it is easy to confuse residual folded noise peaks as pulsar detections as some noise spike candidates can pass most of the validation tests listed. It is not easy to confirm real detections but with care and persistence it can be done. Once comprehensibly verified, it is feasible to add daily folded data sets to improve overall signal-to-noise ratio. Some 13 days of early-morning data collections have been analyzed and B0329+54 pulses recognized based on the 8-point validation scheme described within the SNR range 3.0 to 4.9 (the variation

is due to natural scintillation and/or local RFI). Their arithmetic sum is shown in Figure 16. producing a combined SNR of 10.3. B0329+54 is known to exhibit leading and trailing pulses and further acquisitions might be expected to confirm their presence.

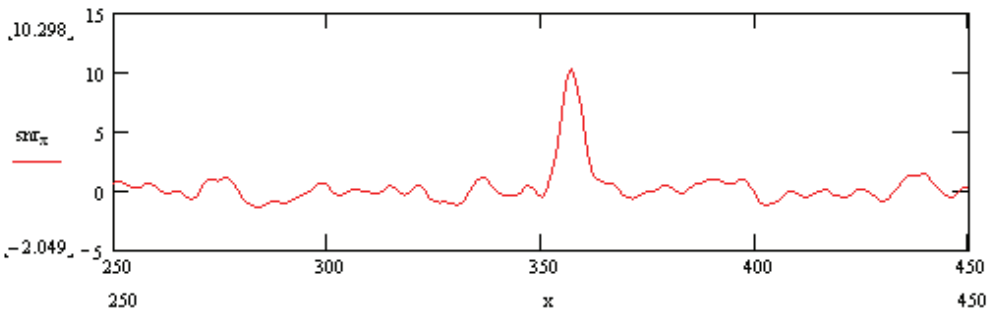

Figure 16. Sum of 13 Days Records, SNR = 10.3

These 13 records have fortunately shown little evidence of serious RFI as most were collected in the benign environment of the early hours of the morning but it has been found that data collected during the daytime and evening hours are more prone to RFI disturbance from cars and computers etc:. The 5-element filter was very effective in removing digital TV RFI. The folding algorithm is known to be very rugged against RFI but it does appear to increase the base noise level, so reducing sensitivity and possibly impair positive detection.
Experience has shown that pulsar detected SNRs above 4.0 can be confidently identified, whereas SNRs around 3.0 require a lot more work. Appendix 3 is a MathCAD summary of the analysis of Dataset 31, taken on 11 October 2017, one of the strongest intercepts made with a topocentric error of +0.35 and a resulting SNR of 4.9. Using the techniques described in this report together with an accurate system clock, an SNR of 2.8 has been confirmed offering the possibility of recognizing pulsar SNRs under good conditions at a lower level. This project may have been blessed with good pulsar scintillation conditions and low local RFI, but the choice of frequency band and antenna was well-rewarded. Had this not been the case, the next move would have been to add a further pair of antennas and a bit more effort made to lower the receiver noise temperature. Most of the work on the data to discover the pulsar signals was devoted to software processing where application of the enhanced, folding algorithm proved to be the key to making them more easily visible.
Finally, it is easy to be fooled by base noise peaks. Pulsar signals differ in several specific properties; they are true pulses, their frequency components are dispersed, they scintillate and finally are wideband. Passing the sum of the tests described still doesn't guarantee pulsar detection at low signal-to-noise ratios and there must be a minimum. The challenge is to push the detection threshold lower.

References

1. Herrmann W. The "Astropeiler Stockert Story" Part 8: Pulsar Observations. SARA Journal, Nov/Dec 2017, p22.
2. East PW, Gancio GM. Amateur Pulsar Detection Using the RTL SDR. SARA Journal, Sep/Oct 2015, p51.
3. Neutron Star Group - Amateur Pulsar Detection http://www.neutronstar.joataman.net/
4. Italian Amateur Radio Station http://iw5bhy.altervista.org/
5. Hawkesbury Radio Astronomy Observatory http://hawkrao.joataman.net/pulsar/index.html
6. Olney S. Challenges for Amateur Pulsar Detection. http://www.neutronstar.joataman.net/technical/amateur_challenges.html
7. Amateur Pulsar Radio Astronomy. http://www.y1pwe.co.uk/RAProgs/Pulsars.html
8. East PW. Quad RTL SDR Receiver. SARA Journal, Sep/Oct 2016, p73.
9. YagiCAD http://www.yagicad.com/yagicad/YagiCAD.htm
10. Interdigital Bandpass Filter Designer http://www.changpuak.ch/electronics/interdigital_bandpass_filter_designer.php
11. Olney S. Topocentric period online calculator http://neutronstar.joataman.net/technical/psr_topo_freq_calc_estimate.html
12. Olney S. Radiometer calculator http://www.neutronstar.joataman.net/technical/radiometer_eqn.html
13. Pulsar Software http://www.y1pwe.co.uk/RAProgs/SWPulsars.zip
14. Osmocom RTL SDR information https://osmocom.org/projects/sdr/wiki/rtl-sdr
15. Radio-Eyes http://www.radiosky.com/
16. SDRSharp software download https://airspy.com/download/

Appendix 1. Control and Data Collection Software[13]

For background, refer to the 'Data Collection' section in the main paper.

Control and Data Collection Software

run_prg_at – used to run data collection and switch modulation software simultaneously at a chosen time.

run_prg_at	Uses PC clock to run any program at a set time.	*run_prg_at* <"program.exe"><hr min sec>

rtlsdr.bat – batch file to run RTL software in parallel.

Command format example:- *run_prg_at* "rtlsdr.bat" 09 00 00

```
start /b rtl_sdr22r  -d11  trial1.bin -N -g 39 -n 20e9 -f  609e6
start /b rtl_sdr22r  -d22  trial2.bin -N -g 39 -n 20e9 -f  611e6
start /b rtl_sdr22r  -d33  trial3.bin -N -g 39 -n 20e9 -f  613e6
```

SwitchMod.py - RF switch modulator control.

Modulates the switch with a random on and off code for up to 10 seconds.

Command format example:- *run_prg_at* "python SwitchMod.py" 09 00 00

```
# pwe SwitchMod.py  02:10:2017
# Adafruit FT232H Breakout board
# Using the Adafruit USB GPIO board to switch modulate a microwave PIN-diode switch
# Data at https://cdn-learn.adafruit.com/downloads/pdf/adafruit-ft232h-breakout.pdf

#Switch modulation program
#Import standard Python time library.
import time
# Import GPIO and FT232H modules.
import Adafruit_GPIO as GPIO
import Adafruit_GPIO.FT232H as FT232H
import random
import sys
# Temporarily disable the built-in FTDI serial driver on Mac & Linux platforms.
FT232H.use_FT232H()
# Create an FT232H object that grabs the first available FT232H device found.
ft232h = FT232H.FT232H()

# Configure digital inputs and outputs using the setup function.
# Note that pin numbers 0 to 15 map to input pins D0 to D7 then output pins C0 to C7 on the board.

ft232h.setup(8, GPIO.OUT)  # Make pin C0 a digital output.

# for-loop turning the switch/LED on and off.

for x in range(0,100):
# Set pin C0 to a high level so the switch/LED turns off.
ft232h.output(8, GPIO.HIGH)
# Sleep for random sub 0.1 second.
time.sleep(random.random()/10)
# Set pin C0 to a low level so the switchLED turns on.
ft232h.output(8, GPIO.LOW)
# Sleep for random sub 0.1 second.
time.sleep(random.random()/10)
#exit leaving the switch on
sys.exit(0)
```

Appendix 2 Data Processing Software[13]

Includes the processes of downsampling/detection, band data timing/correlation and data folding.

Detection Software:

pdetect22.exe carries out amplitude detection and down-sampling of the binary data files.

Command format example: *pdetect22* trial1.bin trial1.txt 2.0 1.0 1

pdetect22.exe	Inputs RTL .bin files, downsamples/square-law detects. Outputs text file of the video integrated detected power - time response. It integrates blocks proportional to the inverse of the video band figure. The divisor figure (normally 1) reduces the analysed file to this factor for test purposes.	*pdetect22* <datfile.bin> <outfile.txt> < RTL data rate (MHz)> <Video Band (kHz)> <File divisor>

This initial downsampling is usually of the order 1000, ensuring much reduced post processing times.

Correlation software:

cor_tim1_nv.exe correlates the initial random modulation in the three RF bands and indicates the relative offset in the samples. Offsets and the initial 10seconds of modulation can be removed with *txttrim2.exe.*

Command format: *cor_tim1_nv* test11.txt test12.txt 1024 16384 10

cor_tim1_nv	Inputs *pdetect22* text files. Takes first block of 'sample length', and correlates this block along the second .txt file and vice versa, to find the correlation peak. Output text file contains the summary. (sample and blocks power 2)	*cor_tim1_nv* <infile1> <infile2> <outfile> <sample length> < block size><No. of blocks tested>
txttrim2	Input a *pdetect22* text file and number of samples to remove from the beginning and end of file to output to a second text file	*txttrim2* <infile.txt> <outfile.txt> <start> <end>
filesum2	Sums four *pdetect22* text files with weighting factors specified by gain entries in the command line. Intended for Quad RTL receiver measurements. Prints gains, mean and rms level of output data.	*filesum2* <infile1> <infile2> <infile3> <infile4> < gain1> <gain2> <gain3> <gain4> <outfile>

Once the three files are trimmed taking into account the adjustment required for de-dispersion and modulation clipping, preferably, equal length files are summed for the following folding process.

Folding software:

The folding software, *rapulsar2_avg2conv.exe* incorporates the SNR enhanced fold algorithm.

Command format: *rapulsar2_avg2conv* test1.txt outtest1.txt 0.001 714 714.45 4.0

rapulsar2_avg2conv	For downsampled/detected .txt files. (from *pdetect22*) Integrates scalar power data synchronously on a timebase set at or very near to the pulsar period. Convolves data with gaussian target. Output text file is the averaged pulse shape at an arbitrary initial phase. Optimum target pulse is 50-70% real	rapulsar2_avg2conv <datfile.txt> <outfile.txt> < downsampled data rate (MHz)> <No. data bins> <Pulsar period (ms)> <nominal pulse width (ms)>
rapulsar2conv	As *rapulsar2_avg2conv* operates on RTL bin files. Outputs a text file that describes the averaged pulse shape. Second column is improved SNR convolved data.	rapulsar2conv <datfile.bin> <outfile.txt> < RTL data rate (MHz)> <No. data bins> <Pulsar period (ms)> <nominal pulse width (ms) >

Appendix 3. MathCad Software

DataCheck.mcd - August 2017 pwe - Input 3-channel band data nominally text files in 1ms steps.
Checks, data quality, data synchronism, half file correlation, band correlation, multi-period folding and period

$x := 0..8192 - 1$ $\quad Max := 12300006$ $\quad Min := 12300000$ $\quad Mm := \frac{Max - Min}{2}$ $\quad Q := 1$

$z := Min..Max - 1$ $\quad Z := 0..Mm - 1$ $\quad Mm = 3.69 \times 10^{6}$ $\quad$ Set 31, data

Band Input Data:

$B1 := READPRN("try311pd.txt")$ $\quad B2 := READPRN("try312pd.txt")$ $\quad B3 := READPRN("try313pd.txt")$

$b1_x := B1_{[(x+X)\cdot Q]}$ $\quad b2_x := B2_{(x+X)\cdot Q}$ $\quad b3_x := B3_{(x+X)\cdot Q}$

$B1d_z := B1_{z+X+29+2+Dd}$ $\quad B2d_z := B2_{z+X+13}$ $\quad B3d_z := B3_{z+X-2-Dd}$

Pulsar Topocentric period
Change numerator for 1/8 ppm variation $\quad Pp \equiv 0$

$$PP \equiv 714.47928714\left(1 + \frac{2.77}{8000000}\right)\cdot\left(1 + \frac{Pp}{1000000}\right)$$

$m1 := 2.2$ $\quad m2 := 0.9$ $\quad m3 := 2.2$

All-band sum: change m factors above to equalise channel amplitudes:

$Sum_z := B1d_z \cdot m1 + B2d_z \cdot m2 + B3d_z \cdot m3$

Raw Data plot - check file synchronism

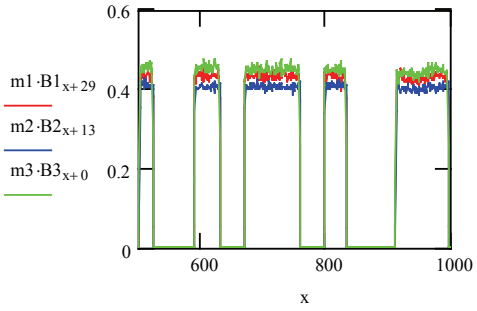

Data plot to check and define m-factors to equalise band contributions

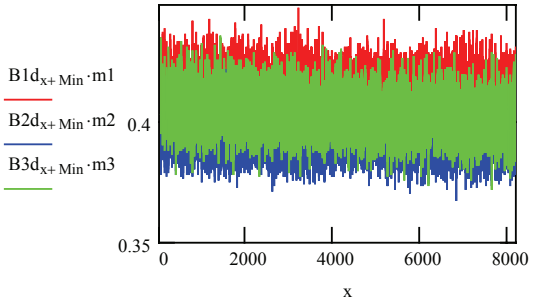

Data plot every Qth data element

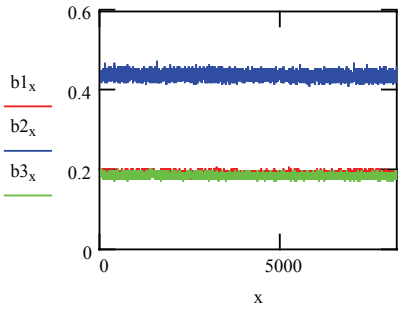

Sum Data plot every Qth data element

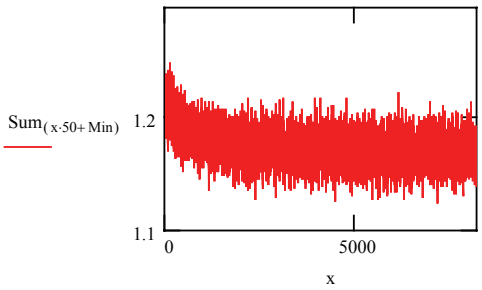

$k := 0..N - 1$ $\quad PPP := M\,PP$

Folding algorithm:

$$mm_z := floor\left[\left(\frac{z}{PPP} - floor\left(\frac{z}{PPP}\right)\right)\cdot N\right]$$

$pmU_k := 0$ $\quad pmL_k := 0$ $\quad pm1_k := 0$ $\quad pm_k := 0$ $\quad pm3_k := 0$

$couU_k := 0$ $\quad couL_k := 0$ $\quad pm2_k := 0$ $\quad cou_k := 0$

Multi-period fold number:

$M \equiv 1$

Number of fold bins:

$N \equiv 715 \cdot M$

$H := \text{floor}\left(\frac{N}{2}\right)$

Offset start value

$X \equiv 12029$

Target shape functions:

Gaussian

$$fe(x, j, d) := \exp\left[-4 \cdot \ln(2)\left(\left(\frac{x - j}{d}\right)\right)^2\right]$$

Triangular

$$ff(x, j, d) := \text{if}\left(j < x < j + d, 1 - \frac{x - j}{d}, 0\right) + \text{if}\left(j \geq x > j - d, 1 - \frac{j - x}{d}, 0\right)$$

Dispersion variable

$Dd \equiv 0$

Target spectrum

$zz := 0 .. (N - 1)$

$a_{zz} := fe\left(zz, \text{floor}\left(\frac{N}{2}\right), 5.0\right)$

$fa := \text{cfft}(a)$

Fold Statistics

$fb1 := \text{cfft}(b1)$

$fb2 := \text{cfft}(b2)$

$fb3 := \text{cfft}(b3)$

Data spectrum

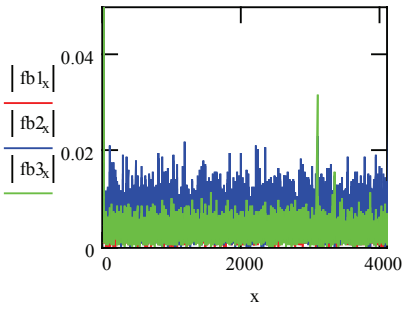

Fold Convolver

$Fco(bdat, bcnt, bno) :=$

for $x \in 0 .. N - 1$

$Oo_x \leftarrow \frac{bdat_x}{bcnt_x}$

$fto \leftarrow \text{cfft}(Oo)$

for $x \in 0 .. N - 1$

$foto_x \leftarrow \left|\frac{fa_x}{fa_0}\right| \cdot fto_x$

$ifto \leftarrow \text{icfft}(foto)$

$mtfo \leftarrow 0$

for $x \in 0 .. N - 1$

$mtfo \leftarrow mtfo + ifto_x$

$mtfo \leftarrow \frac{mtfo - ifto_{bno}}{N - 1}$

$ifto - mtfo$

$Fs(bdat, bcnt, bno) :=$

for $x \in 0 .. N - 1$

$o_x \leftarrow \frac{bdat_x}{bcnt_x}$

$fo \leftarrow \text{cfft}(o)$

$mifo_0 \leftarrow 0$

$mifo_1 \leftarrow 0$

$mifo_2 \leftarrow 0$

$mifo_3 \leftarrow 0$

for $x \in 0 .. N - 1$

$foo_x \leftarrow \left|\frac{fa_x}{fa_0}\right| \cdot fo_x$

$ifo \leftarrow \text{icfft}(foo)$

for $x \in 0 .. N - 1$

$mifo_0 \leftarrow mifo_0 + ifo_x$

$mifo_0 \leftarrow \frac{mifo_0 - ifo_{bno}}{N - 1}$

for $x \in 0 .. N - 1$

$mifo_1 \leftarrow mifo_1 + (ifo_x - mifo_0)^2$

$mifo_1 \leftarrow \sqrt{\frac{mifo_1 - (ifo_{bno} - mifo_0)^2}{N - 1}}$

$mifo_2 \leftarrow \frac{ifo_{bno} - mifo_0}{mifo_1}$

$mifo_3 \leftarrow \frac{mifo_0}{mifo_1}$

$mifo$

Lower half of file

$couL_{(mm_{Z+Min})} := couL_{(mm_{Z+Min})} + 1$

$pmL_{(mm_{Z+Min})} := pmL_{(mm_{Z+Min})} + Sum_{Z+Min}$

Upper half of file

$couU_{(mm_{Z+Min+Mm})} := couU_{(mm_{Z+Min+Mm})} + 1$

$pmU_{(mm_{Z+Min+Mm})} := pmU_{(mm_{Z+Min+Mm})} + Sum_{Z+Min+Mm}$

Half file statistics at bin H: mean,rms,SNR and mean/rms

$$Fs(pmL, couL, H) = \begin{pmatrix} 1.172 \\ 6.224\times 10^{-5} \\ 3.4 \\ 1.883\times 10^{4} \end{pmatrix}$$

$$Fs(pmU, couU, H) = \begin{pmatrix} 1.183 \\ 5.932\times 10^{-5} \\ 3.559 \\ 1.995\times 10^{4} \end{pmatrix}$$

Convolved Spectrum

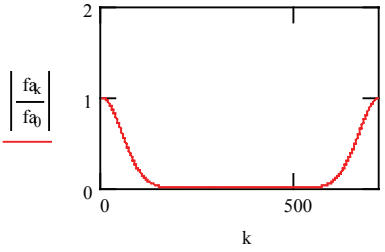

First half file - second half file folding correlation:

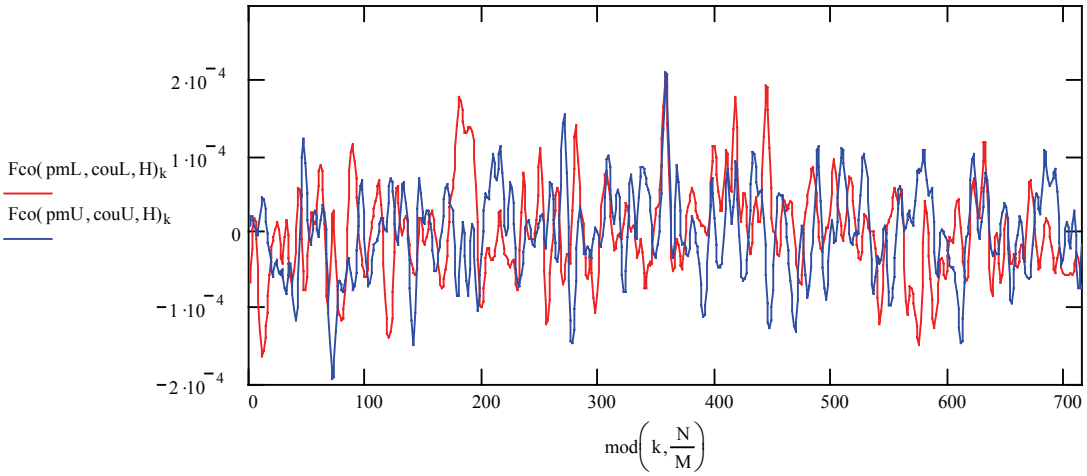

Total SNR statistics

$$pm_{(mm_z)} := pm_{(mm_z)} + Sum_z$$

$$cou_{(mm_z)} := cou_{(mm_z)} + 1$$

Total Band Sum fold - SNR

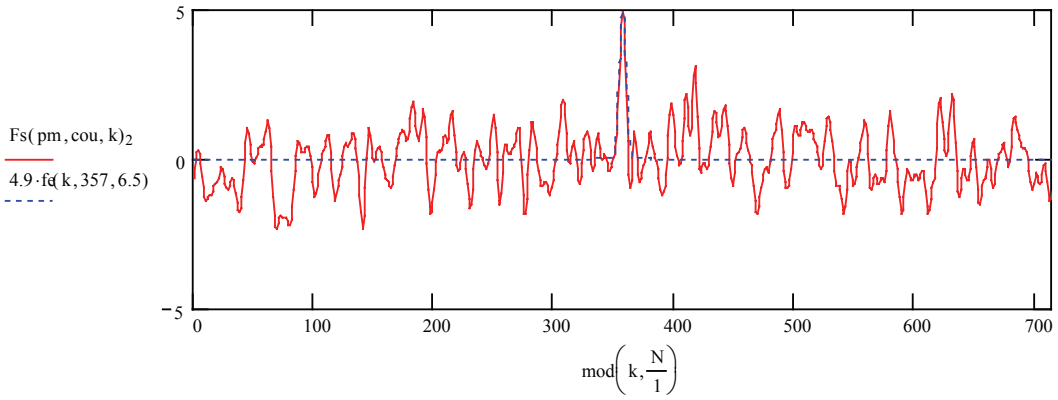

Mean Power: $Fs(pm, cou, H)_1 = 4.308\times 10^{-5}$

All band total SNR: $Fs(pm, cou, H)_2 = 4.893$

Radiometric noise ratio $Fs(pm, cou, H)_3 = 2.734\times 10^{4}$

$$Fs(pm, cou, H) = \begin{pmatrix} 1.178 \\ 4.308\times 10^{-5} \\ 4.893 \\ 2.734\times 10^{4} \end{pmatrix}$$

Band SNR statistics

$$pm1_{(mm_z)} := pm1_{(mm_z)} + m1B1d_z \quad pm2_{(mm_z)} := pm2_{(mm_z)} + m2B2d_z \quad pm3_{(mm_z)} := pm3_{(mm_z)} + m3B3d_z$$

3 - Bands overlapped - de-dispersed - showing correlation

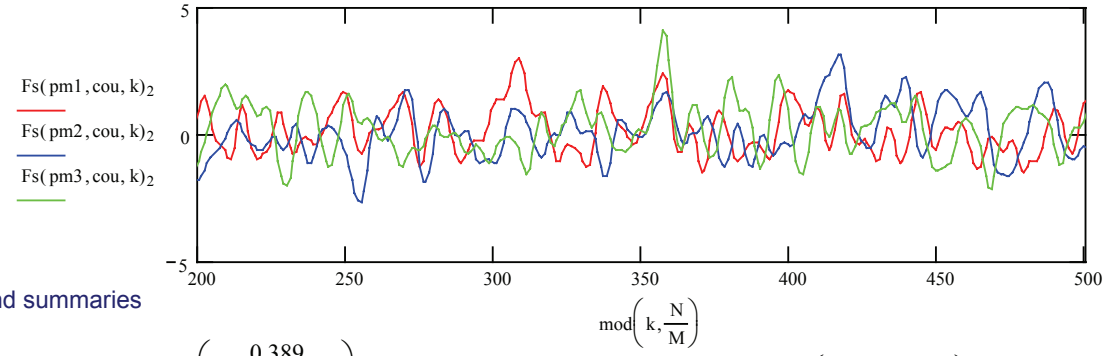

Band summaries

$$Fs(pm1, cou, H) = \begin{pmatrix} 0.389 \\ 2.571\times 10^{-5} \\ 2.368 \\ 1.511\times 10^{4} \end{pmatrix}$$

$$Fs(pm2, cou, H) = \begin{pmatrix} 0.391 \\ 2.248\times 10^{-5} \\ 1.562 \\ 1.741\times 10^{4} \end{pmatrix}$$

$$Fs(pm3, cou, H) = \begin{pmatrix} 0.398 \\ 2.808\times 10^{-5} \\ 4.089 \\ 1.417\times 10^{4} \end{pmatrix}$$

$zm := \frac{Max}{8}$ $zd := 0..7$

1/8ths file folding correlation:

$z6 := 0..zm - 1$ $couz_{0,0} := 0$ $pmz_{0,0} := 0$

$couz(mm_{z6+\,zd\cdot zm}, zd := couz(mm_{z6+\,zd\cdot zm}, zd + 1$

$pmz(mm_{z6+\,zd\cdot zm}, zd := pmz(mm_{z6+\,zd\cdot zm}, zd + Sum_{z6+zd\cdot zm}$

$S_{zd,\,k} := Re(Fco(pmz^{\langle zd \rangle}, couz^{\langle zd \rangle}, H)_k)$

$St_k := \left(\sum_{zd} S_{zd,\,k}\right) \cdot \frac{1}{\sqrt{8}}$

Ovelapped 1/8th of file showing all section correlation

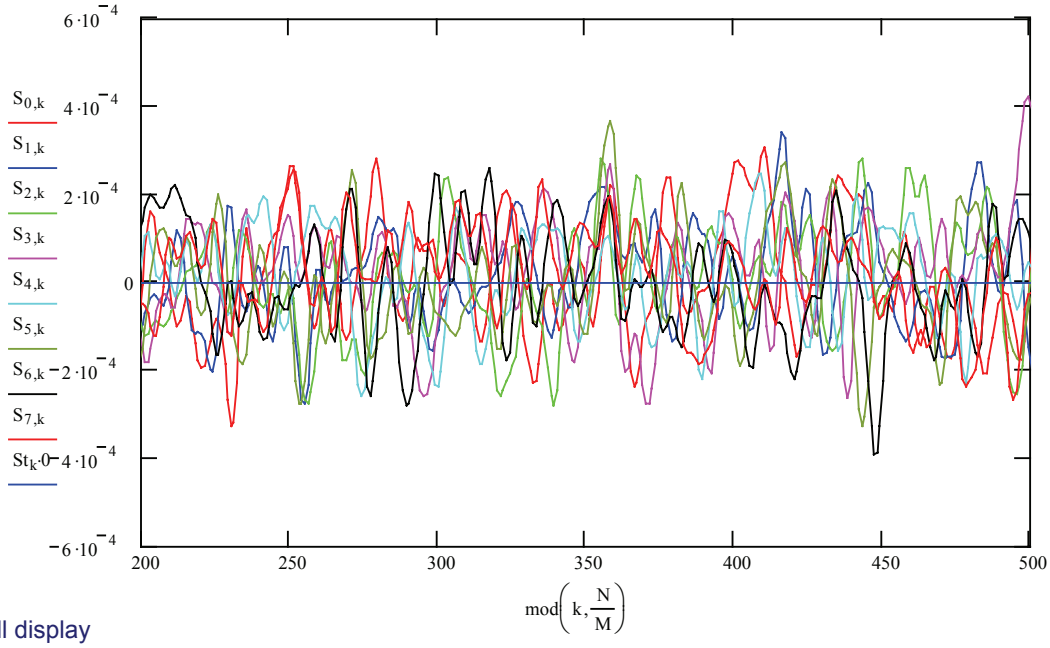

Waterfall display

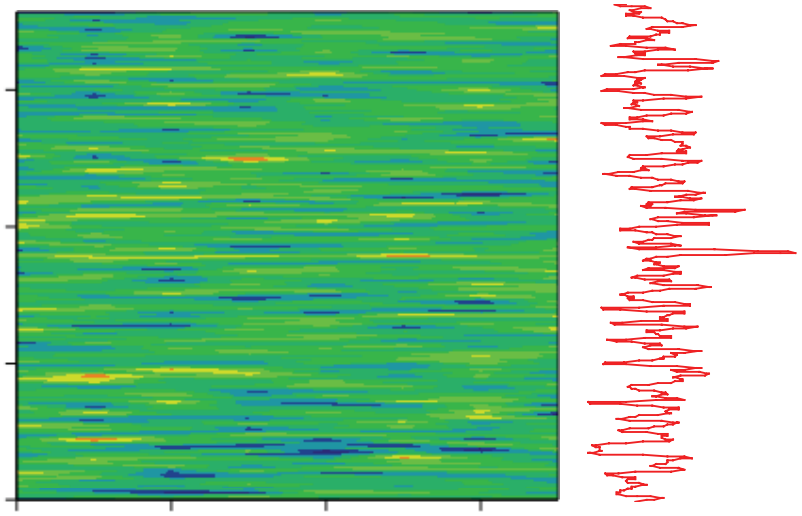

$Fs(pm, cou, k)_2$

S

Appendix 4. Yagi Antenna Design

17-element Yagi - YagiCAD6 6.2 by Paul McMahon VK3DIP

Frequency: 611MHz

Design Table:

Element	Length (m)	Position (m)	Diameter (m)	Material
Reflector	0.269	0.000	0.006	Aluminium
Di-pole	0.255	0.115	0.006	Aluminium
Director 1	0.237	0.155	0.006	Aluminium
Director 2	0.235	0.245	0.006	Aluminium
Director 3	0.232	0.353	0.006	Aluminium
Director 4	0.230	0.479	0.006	Aluminium
Director 5	0.227	0.619	0.006	Aluminium
Director 6	0.224	0.770	0.006	Aluminium
Director 7	0.222	0.929	0.006	Aluminium
Director 8	0.220	1.094	0.006	Aluminium
Director 9	0.218	1.267	0.006	Aluminium
Director 10	0.218	1.447	0.006	Aluminium
Director 11	0.216	1.634	0.006	Aluminium
Director 12	0.215	1.825	0.006	Aluminium
Director 13	0.214	2.019	0.006	Aluminium
Director 14	0.213	2.217	0.006	Aluminium
Director 15	0.212	2.419	0.006	Aluminium

Note: Positions measured from the first reflector element

Boom: 0.0254 m square, 2.7 m long.
Elements in 6 mm central holes, held by self-tapping steel screws.
Driven di-pole mounted in 10 mm perspex tube insulation

Input impedance: 44.59 + j0.74 ohms
Forward gain: 16.9 dBi
Front to back ratio: 23.2 dB
3 dB Beamwidth E: 27°
3 dB Beamwidth H: 28.5°

Appendix 5

5-Element Interdigital Filter

Interdigital Bandpass Filter, based on work of Jerry Hinshaw, Shahrokh Monemzadeh (1985) and Dale Heatherington (1996). www.changpuak.ch/electronics/interdigital_bandpass_filter_designer.php

Design data for a 5 section interdigital bandpass filter.

Center Frequency	:	611 MHz
Passband Ripple	:	0.5 dB
System Impedance	:	50 Ohm
Cutoff Frequency	:	608 MHz and 614 MHz
Bandwidth (3dB)	:	6.4 MHz
Fractional Bandwidth	:	0.0098
Filter Q	:	96.136

Estimated Qu : 1719.66
Loss, based on this Qu : 2.162 dB
Passband Delay : 223.128 ns

Quarter Wavelength : 122.66 mm or 4.829 inch
Length interior Element : 116.62 mm or 4.591 inch
Length of end Element : 116.81 mm or 4.599 inch
Ground plane space : 25.4 mm or 1.000 inch
Rod Diameter : 6 mm or 0.236 inch
End plate to center of Rod : 15 mm or 0.591 inch
Tap to shorted End : 3.75 mm or 0.148 inch
Impedance end Rod : 98.069 Ohm
Impedance inner Rod : 101.003 Ohm
Impedance ext. line : 50.000 Ohm

**** Dimensions, mm (inch) ****

#	End to Center	Center-Center	G[k]	Q/Coup
0	0.00 (0.000)			
1	15.00 (0.591)	43.54 (1.714)	1.706	0.652
2	58.54 (2.305)	45.27 (1.782)	1.230	0.534
3	103.81 (4.087)	45.27 (1.782)	2.541	0.534
4	149.09 (5.869)	43.54 (1.714)	1.230	0.652
5	192.63 (7.584)	0.00 (0.000)	1.706	1.807
6	207.63 (8.174)			

**** Box inside dimensions ****
Height : 122.66 mm or 4.829 inch
Length : 207.63 mm or 8.174 inch
Depth : 25.40 mm or 1.000 inch

Construction:

Sides: 1" by 1/4" Aluminium bar drilled and assembled using self-tapping screws.
Top/Bottom: 1/16" Aluminium plate drilled and assembled using self-tapping screws.
Elements: 6 mm Copper rod, slotted in 6 mm holes and held by self-tapping screws.
Tuning screws: M6 bolts with locking nuts